ACS Catalysis

pubs.acs.org/acscatalysis Letter

Highly Regio- and Stereoselective Markovnikov Hydrosilylation of Alkynes Catalyzed by High-Nuclearity {Co_{14}} Clusters

Jun-Song Jia, Yan Cao, Tai-Xue Wu, Ye Tao, Ying-Ming Pan,* Fu-Ping Huang,* and Hai-Tao Tang*

Cite This: *ACS Catal.* 2021, 11, 6944−6950 Read Online

ACCESS | Metrics & More | Article Recommendations | Supporting Information

ABSTRACT: This work developed three high-nuclearity {Co_{14}} clusters of **C1**−**C3** with inner [Co_8] backbone fixed by six ambient $CoCl_2$ species. The catalyst **C1** exhibited highly regio- and stereoselective hydrosilylation of alkynes with primary and secondary silane to produce α-vinylsilanes. More importantly, **C1** shows high regioselectivity for electronically unbiased alkyl alkynes, and the α-selectivity of some alkyl alkynes has not been achieved in previous reports. Leaching tests and reusability proved that the reaction is a heterogeneous process.

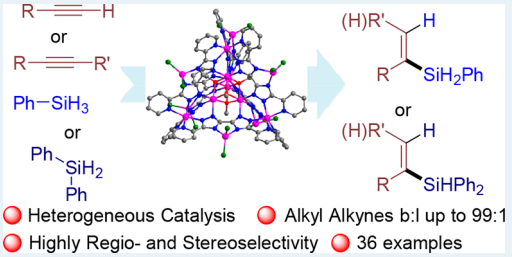

KEYWORDS: *high-nuclearity clusters, hydrosilylation, regioselectivity, aliphatic alkyne, heterogeneous catalyst*

Silyl-substituted alkenes[1] are attractive building blocks because they are innocuous, highly stable, easy to handle and store, and are widely used in modern intermediates in organic synthesis,[2] polymeric organosilicon materials,[3] and fine chemistry.[4,3b] Among the synthetic paths to vinylsilanes, the transition metal-catalyzed hydrosilylation of alkynes is 100% atom efficient, straightforward, and a convenient route to obtain valuable vinylsilanes.[5] A challenge in the hydrosilylation of alkynes is controlling regio- and stereoselectivity because these reactions can potentially produce mixture products, such as β-(*Z*)-, β-(*E*)-, and α-vinylsilanes, and excess hydrosilylation products (Scheme 1).[6]

Scheme 1. Possible Product of Terminal Alkyne Hydrosilylation

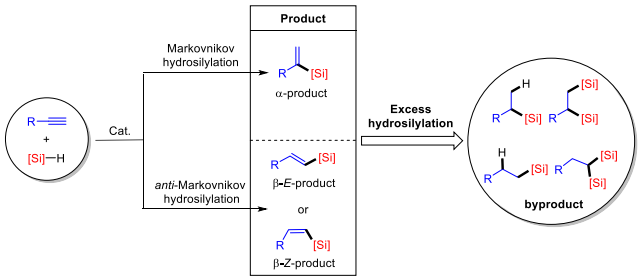

The regioselective and stereoselective hydrosilylation of alkynes has been well controlled by using R_3SiH as a silicon reagent.[7] However, when more active $RSiH_3$ is used as a silicon reagent, α-selective hydrosilylation of alkynes is still a challenge.[6] Earth-abundant metals are important for the sustainable future of organic synthesis and manufacturing because of their low cost, low toxicity, and abundance.[8] The use of earth-abundant metals, such as Co, for hydrosilylation is becoming increasingly popular. In 2016, Lu and Huang independently reported the highly selective cobalt-catalyzed α-selective hydrosilylation of alkynes with Ph_2SiH_2 to achieve α-vinylsilanes.[6d,9] Unfortunately, Lu and Huang did not report the α-selective hydrosilylation of alkynes that uses $RSiH_3$ as a silicon reagent. Moreover, the α-selectivity of alkyl alkynes was unsatisfactory (branched:linear [b:l] = 69:31−87:13, Scheme 2a1, a2). In 2018, Yang developed the highly α-selective hydrosilylation of alkynes by using $PhSiH_3$ to access α-vinylsilanes.[10] However, the regioselectivity of alkyl alkynes was poor (b:l = 45:55, Scheme 2a3). In 2019, Jin et al. used NN bidentate ligand to achieve the α-selective hydrosilylation of alkynes by using $PhSiH_3$ and Ph_2SiH_2 as silicon reagents.[11] The α-selectivity of this reaction was also limited to alkyl alkynes (b:l = 63:37−85:15, Scheme 2a4). Wangelin and Chen reported the α-selective hydrosilylation of alkynes by using $PhSiH_3$ or Ph_2SiH_2 as silicon reagent.[12] However, their b:l ratios were limited to alkyl alkynes (b:l = 73:28−78:22). Therefore, the development of α-selective hydrosilylation reactions by using electronically unbiased alkynes especially for aliphatic alkynes as substrates in a catalytic manner is challenging.

Our group is committed to solve the selectivity of organic reactions that cannot be completely solved in homogeneous catalytic reactions with heterogeneous catalysts. Reports on the hydrosilylation of alkynes under heterogeneous catalysis are

Received: May 2, 2021
Revised: May 26, 2021
Published: June 1, 2021

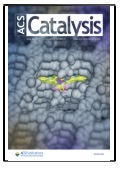

https://doi.org/10.1021/acscatal.1c01996
ACS Catal. 2021, 11, 6944−6950

Scheme 2. Hydrosilylation of Terminal Alkyne

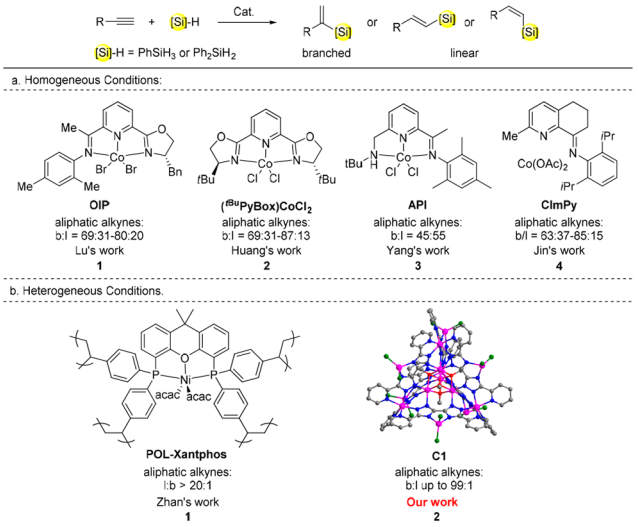

limited. In 2012, Ramón et al. reported the hydrosilylation of internal alkynes by using $PtO/PtO_2-Fe_3O_4$ as a heterogeneous catalyst, but the regioselectivity of terminal alkynes is unsatisfactory.[13] In 2018, Zhan et al. reported the use of porous organic polymers−Xantphos as a heterogeneous catalyst to achieve the high β-*E*-selective hydrosilylation of terminal alkynes. However, no α-selective hydrosilylation is reported (Scheme 2b1).[14] To the best of our knowledge, the α-selective hydrosilylation of terminal alkynes under heterogeneous conditions has not been reported yet.

The synthesis of high-nuclearity 3d transition metal coordination clusters is currently a major topic of interest. Such metals include Fe_{168}, Mn_{84}, Co_{36}, Ni_{34}, and Cu_{147},[15] and their various remarkable structures and rich functions in single-molecule magnets, optics, electricity, biology, and catalysis.[16−20] The challenge in searching for new atomically precise catalysts in organic reactions is the control of regio- and stereoselectivity to produce selective products. Also, the easy destruction and/or difficult recycling in low-nuclearity homogeneous metal catalysts and the shape and/or size limit in heterogeneous metal−organic frameworks/metal−ligand cluster hosts catalysts with/without endo-open-metal-sites (OMS) should be addressed.[21,22] Thus, heterogeneous selective high-nuclearity cluster-base catalysts with rich exo OMS should be developed.

In this work, three high-nuclearity $\{Co_{14}\}$ clusters of **C1**−**C3**, were obtained from three derivative 5,5′-di(pyridin-2-yl)-3,3′-bi(1,2,4-triazole) ligands **L1**, **L2**, and **L3** (Scheme 3), respectively (synthetic methods and crystal data are shown in the Supporting Information). Single-crystal X-ray analysis showed that **C1**−**C3**, which had similar structural features, had a tetrahedral $[Co_8]$ inner skeleton fixed by ligands (**L1**−**L3**), thereby further chelating six $CoCl_2$ species as exo-OMS on the edges. **C1**−**C3** were used as heterogeneous catalysts to achieve the high regio- and stereoselective hydrosilylation of alkynes. The reaction had a wide scope of alkynes (36 examples) and good yields. The α-selective hydrosilylation of challenging alkyl alkynes achieved moderate to excellent regioselectivity (b:l up to 99:1). Compared with other activating reagents (e.g., RMgX, RLi, $LiAlH_4$, and $NaBHEt_3$), NaO^tBu was safe, stable in air/moisture, easy to handle, and inexpensive.

Scheme 3. Catalysts L1−L3 and C1−C3

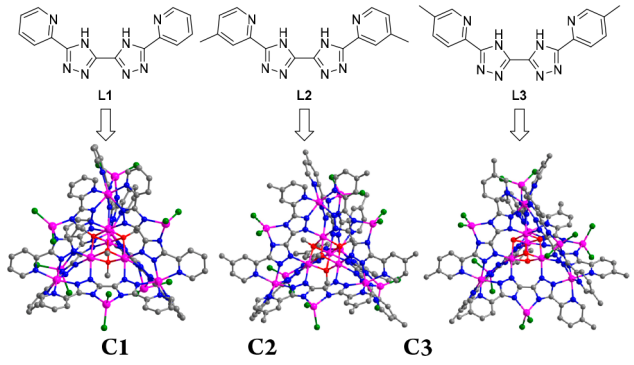

Single-crystal X-ray diffraction studies showed that **C1**−**C3** consisted of a $[Co_{14}(\mu_3-OH/OCH_3)_4(L_x)_6Cl_{12}]$ (here x = 1 for **C1**, 2 for **C2**, and 3 for **C3**, respectively) cluster and different lattice solvents. The $[Co_{14}(\mu_3-OH/OCH_3)_4(L_x)_6Cl_{12}]$ cluster of **C1**−**C3** had a stable $[Co_8]$ backbone composed with an inner cuboidal $[Co_4(\mu_3-OH/OCH_3)_4]$ core, which consisted of four octahedral Co atoms in distorted octahedral CoN_3O_3 environments held together tightly by four μ_3-CH_3O anions in **C1**−**C2** and four μ_3−OHanions in **C3**, respectively. The $[Co_4(L_x)_6]$ periphery consisted of six L_x ligands arranged into a distorted tetrahedron wrapping the $[Co_4(\mu_3-OH/OCH_3)_4]$ core tightly and four Co atoms in CoN_6 environments lying at the vertices of the distorted tetrahedron. Interestingly, the remaining six Co(II) ions in the distorted N_2Cl_2 tetrahedron geometry were chelated by six L_x ligands and 12 Cl anions. Therefore, the potential active sites (six coordinately unsaturated $CoCl_2$ species as exo-OMS) were fixed on the edges of the tetrahedral $[Co_8]$ inner backbone.

The alkyne hydrosilylation was started by evaluating the conditions for the reaction between phenylacetylene (**1a**) and $PhSiH_3$ (**2a**, Table 1). The activity of $CoCl_2$ with three dpbt ligands **L1**−**L3** in catalyzing the hydrosilylation of phenylacetylene with $PhSiH_3$ was tested. Then, 2 mol % ligands **L1**−**L3**, 1.8 mol % $CoCl_2$, 3 mol % activator NaO^tBu, and tetrahydrofuran (THF) as solvent were used. The reaction was carried out for 4 h at room temperature under Ar protection. Unfortunately, only trace of target products can be observed under these conditions (entries 1−3 in Table 1).

Table 1. Screening of Catalyst[a]

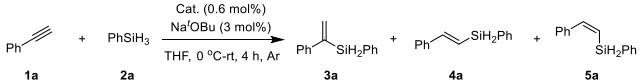

entry	catalyst	yield (%)[b]	ratio (**3a**:**4a**:**5a**)[c]
1	**L1**+$CoCl_2$	trace	-
2	**L2**+$CoCl_2$	trace	-
3	**L3**+$CoCl_2$	trace	-
4	**C1**	86	99:1:nd
5	**C2**	82	98:2:nd
6	**C3**	80	93:5:2

[a]Reaction conditions: phenylacetylene (0.5 mmol), $PhSiH_3$ (0.6 mmol), catalyst (0.6 mol %), NaO^tBu (3 mol %), THF (2 mL), 0 °C to rt, 4 h. [b]Isolated yield. [c]Determined using ^1H NMR spectroscopy.

A remarkable increase in the isolated yield under the above reaction conditions was achieved when high-nuclearity $\{Co_{14}\}$

https://doi.org/10.1021/acscatal.1c01996
ACS Catal. 2021, 11, 6944−6950

cluster **C1** was used as catalyst (entry 4, Table 1). The **C1** catalyst showed excellent regioselectivity (**3a**:**4a** = 99:1), as shown by the results of ^{1}H NMR spectroscopy. The hydrosilylation of phenylacetylene with $PhSiH_3$ was tested using high-nuclearity clusters **C2** and **C3** as catalyst. Compared with those of **C1**, the regioselectivity and yield of **C2** and **C3** were slightly reduced (entries 5−6, Table 1). The reason for these results (entries 1−6, Table 1) may be that it is difficult for **L1**−**L3** and $CoCl_2$ to form a single catalyst to promote the reaction. Cluster **C1**−**C3** already has a stable coordination structure of "ligand + metal", so it can efficiently catalyze the reaction. Catalyst loading, activator, solvent, and other reaction conditions were screened (Supporting Information). The standard conditions chosen were alkynes (0.5 mmol), $PhSiH_3$ (0.6 mmol), **C1** (0.6 mol %), and Na^{t}OBu (3 mol %) in a solution of THF (0.25 M) at 0 °C to room temperature for 4 h.

The scope of various alkynes that underwent this high-nuclearity $\{Co_{14}\}$ cluster catalyzed through α-selective hydrosilylation was studied using **C1** as the heterogeneous catalyst. Results are summarized in Table 2. Overall, a wide range of

Table 2. Scope of Alkynes for the Hydrosilylation Reaction with $PhSiH_3$[a]

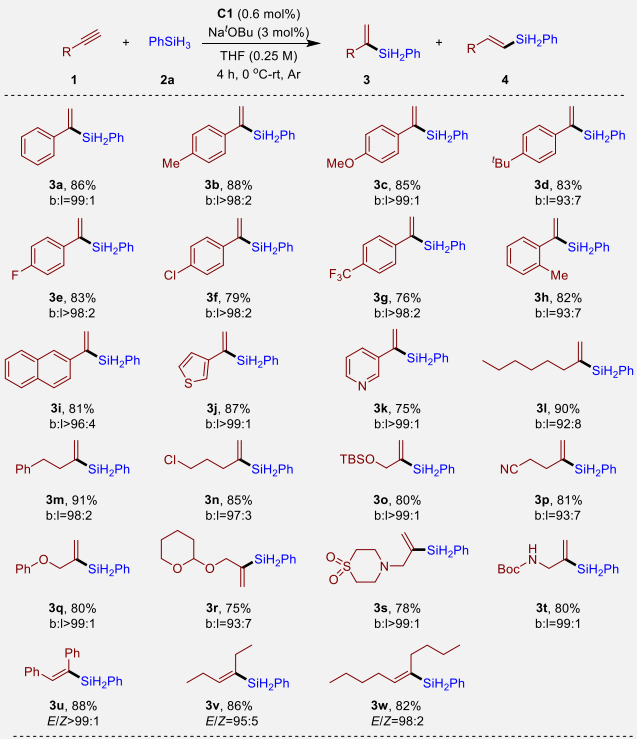

[a]Conditions: **1** (0.5 mmol), $PhSiH_3$ (0.6 mmol), **C1** (0.6 mol %), Na^{t}OBu (3 mol %) in THF (0.25 M), isolated yield. The value of b:l and *E*/*Z* was determined using ^{1}H NMR spectroscopy.

electron-donating or electron-withdrawing substituent aryl alkynes underwent the reaction with $PhSiH_3$. The corresponding hydrosilylation product had good yield and excellent regioselectivities (b:l up to 99:1, **3a**−**3i**). *Para*-electron-donating substituted phenylacetylenes, such as methyl (**1b**) and methoxy (**1c**), could react well with good yield and excellent regioselectivities. *Para*-halogen-substituted phenylacetylenes (**1e**−**1g**) resulted in α-vinylsilanes in moderate to good yield with high regioselectivity (b:l > 98:2) without dehalogenation byproducts. The α-selectivities of *para*-*tert*-butyl alkyne (**1d**), *ortho*-methyl alkyne (**1h**), and 2-naphthyl alkyne (**1i**) were slightly reduced. This result might be due to the steric hindrance that the regioselectivity was slightly reduced. Heteroaromatic alkynes, such as 2-ethynylthiophene (**1j**) and 3-ethynylpyridine (**1k**), proceeded smoothly to deliver the corresponding hydrosilylation product with moderate yield and excellent regioselectivities (b:l > 99:1).

Given that the regioselectivity of the electronically unbiased alkyl alkynes α-selective hydrosilylation is difficult to control, alkyl alkyne hydrosilylation remains a challenge. 1-Octyne (**1l**) was chosen as the alkyne substrate reaction with $PhSiH_3$ to test the selectivity of the catalyst for alkyl alkynes. The value of b:l product was up to 92:8 and 90% isolated yield. The hydrosilylation of other alkyl alkynes, such as 4-phenyl-1-butyne (**1m**) and 5-chloro-1-pentyne (**1n**), also resulted in good yield and excellent regioselectivities (b:l up to 98:2). Subsequently, the hydrosilylation of a series of heteroaliphatic alkynes, such as those containing TBSO (**1o**), cyano (**1p**), ether (**1q**), acetal (**1r**), sulfone (**1s**), and protected primary amine (**1t**), were tested. All hydrosilylation products showed moderate to good yield and high regioselectivities (b:l > 93:7). Furthermore, internal alkynes 1,2-diphenylethyne (**1u**), 3-hexyne (**1v**), and 5-decyne (**1w**) were tolerated, providing *syn*-addition products in good yield (*E*:*Z* up to 99:1).

This catalyzed hydrosilylation was examined with a secondary hydrosilane Ph_2SiH_2 (**2b**) in Table 3. Under standard conditions, the reaction of Ph_2SiH_2 with phenylacetylene (**1a**) resulted in 86% isolated yield and high regioselectivity (b:l > 96:4) of product **7a**. *Ortho*-, *meta*-, and *para*-electron-donating substituted or electron-accepting substituted phenylacetylenes could react well with good yields

Table 3. Scope of Alkynes for Hydrosilylation Reaction with Ph_2SiH_2[a]

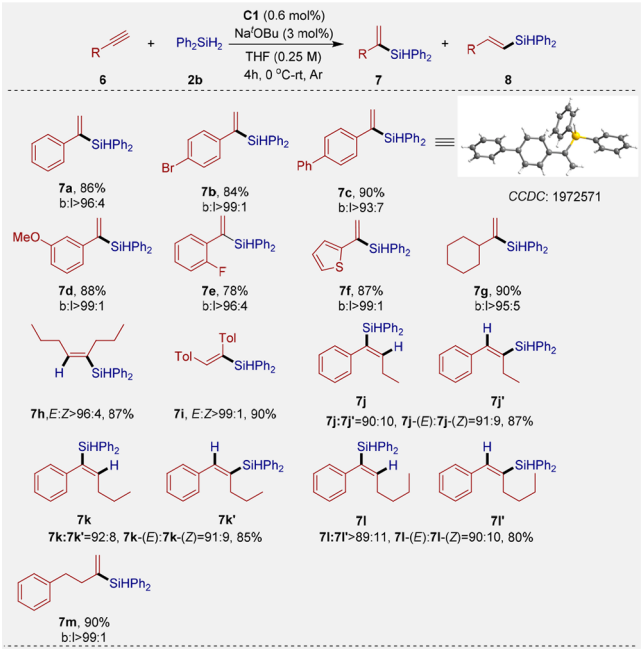

[a]Conditions: **1** (0.5 mmol), Ph_2SiH_2 (0.6 mmol), **C1** (0.6 mol %), Na^{t}OBu (3 mol %) in THF (0.25 M), isolated yield, the ratio of b:l and *E*/*Z* determined using ^{1}H NMR.

https://doi.org/10.1021/acscatal.1c01996
ACS Catal. 2021, 11, 6944−6950

(**7b**−**7e**) and high regioselectivities (b:l > 93:7). The structure of **7c** was further confirmed via X-ray crystallography. The heteroaromatic terminal alkyne 3-ethynylthiophene typically provided good isolated yield and excellent regioselectivitity (**7f**, b:l > 99:1). The hydrosilylation of 1-ethynylcyclohexane provided the desired α-vinylsilane **7g** in high yield with excellent regioselectivity (b:l > 95:5). The hydrosilylation of symmetric dialkylalkye 4-octyne (**6h**) and 1,2-*di*-*p*-tolylethyne (**6i**) resulted in addition products (**7h** and **7i**) with high stereoselectivity (*E*:*Z* up to 99:1, determined using ^{1}H NMR spectroscopy). The asymmetric internal alkynes were suitable for this method to produce **7j**−**7l** with 80%−87% yield and high regioselectivity and stereoselectivity (*E*:*Z* > 90:10). Finally, we also obtained the product **7m** with satisfactory yield and selectivity.

The hydrosilylation of **1a** (5 mmol) with **2a** (6 mmol) was performed under standard conditions to demonstrate the practical utility of this methodology. Results showed that 0.82 g **3a** was obtained in 78% isolated yield with excellent regioselectivity (b:l > 98:2; Scheme 4, eq 1) and the substrate

Scheme 4. Practicality of the $\{Co_{14}\}$ Cluster

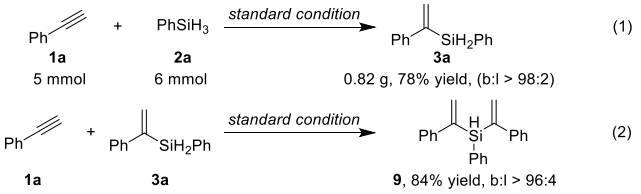

1a was completely consumed. The further conversion of the synthesized α-vinylsilane is a topic of interest in the present work. Under standard conditions, phenylacetylene (**1a**) reacted with **3a**, and the corresponding divinylsilanes (**9**) were achieved with moderate yield and excellent regioselectivity (Scheme 4, eq 2).

As shown in Figure 1, a leaching experiment was performed to investigate whether the reaction was homogeneous or

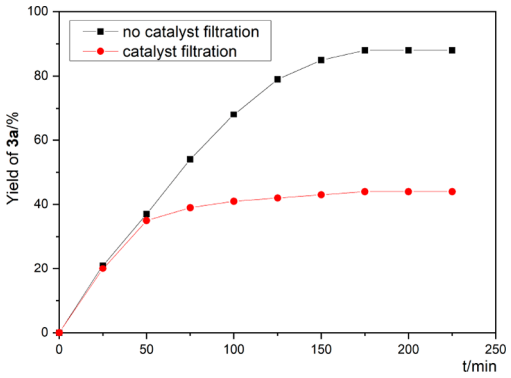

Figure 1. Reaction time examination and leaching test for the hydrosilylation of phenylacetylene with $PhSiH_3$.

heterogeneous. When the hydrosilylation reaction of phenylacetylene with $PhSiH_3$ was carried out for 50 min, the ^{1}H NMR yield was 37%. When the reaction was continued for 4 h, the final ^{1}H NMR yield was 86%. When the reaction was carried out for 50 min, the catalyst was removed by filtration, and the solution was further reacted under the same conditions for 4 h. The final ^{1}H NMR yield was 44%. In addition, by washing and post-treatment of the used catalyst, we realized the four times recycling of the cluster catalyst (Figure 2). Both leaching and cycle test demonstrated that the reaction was a heterogeneously catalyzed process.

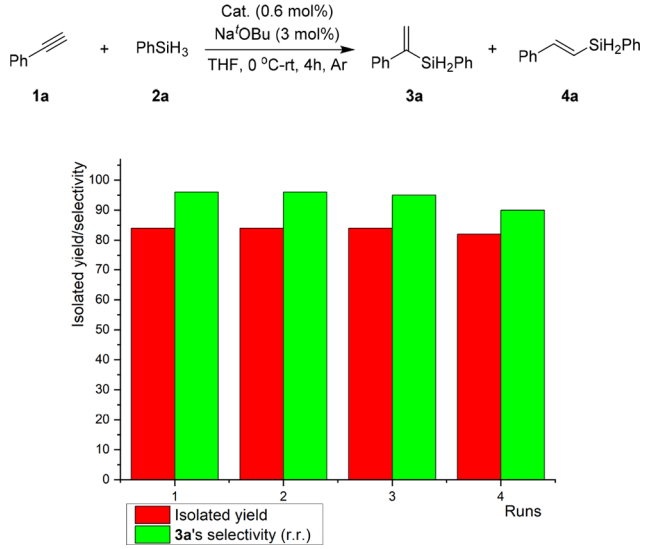

Figure 2. Cycle experiment.

We completed the deuterium-labeling experiment of 4-phenyl-1-butyne (**1m**) and Ph_2SiH_2 to obtain some insights into the α-selective hydrosilylation of alkynes catalyzed by this cluster. Results are shown in Scheme 5. Under standard

Scheme 5. Deuterium-Labeling Experiments

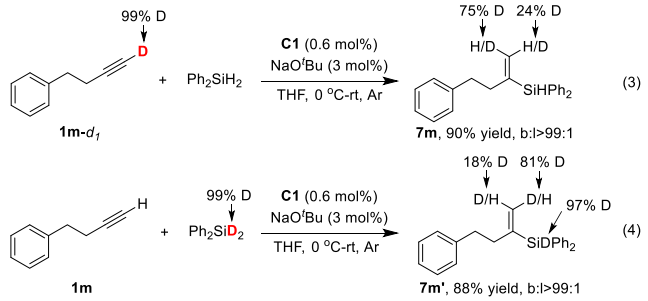

conditions, the reactions of deuterated **1m**-d_1/Ph_2SiH_2 (eq 3 in Scheme 5) and **1m**/Ph_2SiD_2 (eq 4 in Scheme 5) obtained deuterated **7m** with good isolated yield and α-selectivity (b:l > 99:1). The stereoselectivity was *E*:*Z* = 75:25−82:20, which was lower than the stereoselectivity of internal alkynes. This finding might be caused by the partial H/D exchange in the product **7m**.[23] We also tested the reaction of **1a**/Ph_2SiD_2 and deuterated **1a**-d_1/Ph_2SiH_2 under standard conditions, and results were similar to that in Scheme 5 (see Supporting Information). The distribution of deuterium is ill-defined for phenylacetylene. Probably, the more acidic terminal acetylene causes some H/D exchange reaction under the reaction conditions (see Supporting Information).

In order to explain the selectivity of the reaction, Density Function theory (DFT) calculation was carried out. With DFT method, we have optimized the geometries of the subunits of catalysts **C1**, **C2**, and **C3**, as well as the geometries loosing the chlorine ligands (Figure S4 in Supporting Information). Upon the optimized structures were the Mulliken charge derived. As

https://doi.org/10.1021/acscatal.1c01996
ACS Catal. 2021, 11, 6944−6950

for the subunits **C1**, **C2**, and **C3**, we found the charge of cobalt of **C1** (0.380 eV) was a bit higher than those of **C2** (0.365 eV) and **C3** (0.362 eV). So does the trend for the geometries of **C1**, **C2**, and **C3** loosing the chlorine ligands. For terminal alkynes, since the electron cloud density of β-C is higher, the catalyst with more positive charge is easier to form branched products. We also analyzed the natural orbitals for the subunits **C1**, **C2**, and **C3**. we found the gap between the highest occupied molecular orbital (HOMO) and lowest unoccupied molecular orbital (LUMO) for **C1** (72.99 KJ·mol^{-1}) was much lower than those of **C2** (76.40 KJ·mol^{-1}) and **C3** (76.93 KJ·mol^{-1}) (Figure S5 and S6). The smaller gap suggest it is more reactive when interacting with other reactants. The LUMO−HOMO gap of **C1** was lower than those of **C2** and **C3** suggested that the selectivity of **C1** was superior to those of **C2** and **C3**. This is because the smaller gap means an easier way for the electron transition. When the reactant was absorbed by the catalyst, electron transition may occur to trigger the reaction. Thus, the easier for the electron to transfer, the easier for the reaction to occur, and the better selectivity is illustrated. In addition, we computed the adsorption energies between SiH_4 and the catalysts **C1**, **C2**, and **C3** (Table S13). The lower the adsorption energy, the easier the reaction will proceed. Moreover, the Si−H bond in the complex of SiH_4-**C1** is easier to extend from 1.478 to1.584 Å. The extension of Si−H bond was not observed in the other two complexes.

According to Figure 1, the reaction can be regarded almost as a zero-order reaction to both substrates. Thus, this result suggests the rate-limiting step to be the event on the catalyst. On the basis of the results of the selectivity of internal alkynes in our experiments (*syn* H/[Si] addition), deuterium-labeling experiments, and related reports on cocatalyzed alkyne and alkene hydrosilylation reactions,[24,9] we proposed a possible reaction process (Scheme 6). The catalytic process is carried

Scheme 6. Proposed Reaction Mechanisms of Hydrosilylation Catalyzed by {Co_{14}} Clusters

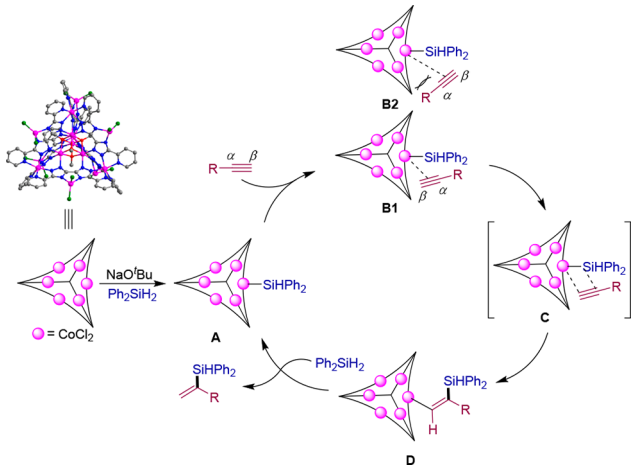

out by a crystalline catalyst. First, under the action of the base NaO^{t}Bu, the $CoCl_2$ in the high-nuclearity cluster reacted with phenylsilane to obtain a low-valent cobalt silyl intermediate **A**, which could further integrate with the carbon−carbon triple bond of alkynes to generate the intermediate **B**. As β-C in the terminal alkynes was more negative than α-C, the positively charged cobalt in the cluster catalyst reacted with β-C first. From the perspective of steric effect, the structure of **B1** was favorable. Therefore, the product with α-regioselectivity was the main product. Subsequently, alkynes underwent the selective 1,2-insertion of Co−Si bonds to form Co alkenyl species **D** and then reacted with Ph_2SiH_2 to form α-selective products and regenerate **A**. In addition, the intermediate **D** underwent the Crabtree−Ojima−type[25] isomerization to generate α-selective products.

In conclusion, a high-nuclearity {Co_{14}} cluster **C1** was developed, showing highly regio- and stereoselective properties in the hydrosilylation of alkynes with primary and secondary silane to produce α-vinylsilanes. The reaction had broad substrate adaptability and good yields. **C1** could achieve high regioselectivity for alkyl alkynes, and the α-selectivity of some alkyl alkynes had not been achieved in previous reports. Leaching tests and reusability of **C1** proved that the reaction was a heterogeneous process.

■ ASSOCIATED CONTENT

Supporting Information

The Supporting Information is available free of charge at https://pubs.acs.org/doi/10.1021/acscatal.1c01996.

Experimental procedure, characterization data, and copies of ^{1}H and ^{13}C NMR spectra (PDF)
Crystallographic data for **7c** (CIF)
Crystallographic data for **C1** (CIF)
Crystallographic data for **C2** (CIF)
Crystallographic data for **C3** (CIF)

■ AUTHOR INFORMATION

Corresponding Authors

Hai-Tao Tang − *State Key Laboratory for Chemistry and Molecular Engineering of Medicinal Resources, School of Chemistry and Pharmaceutical Sciences of Guangxi Normal University, Guilin 541004, People's Republic of China;* orcid.org/0000-0001-7531-0458; Email: httang@gxnu.edu.cn

Fu-Ping Huang − *State Key Laboratory for Chemistry and Molecular Engineering of Medicinal Resources, School of Chemistry and Pharmaceutical Sciences of Guangxi Normal University, Guilin 541004, People's Republic of China;* orcid.org/0000-0003-4227-9815; Email: huangfp2010@163.com

Ying-Ming Pan − *State Key Laboratory for Chemistry and Molecular Engineering of Medicinal Resources, School of Chemistry and Pharmaceutical Sciences of Guangxi Normal University, Guilin 541004, People's Republic of China;* orcid.org/0000-0002-3625-7647; Email: panym@mailbox.gxnu.edu.cn

Authors

Jun-Song Jia − *State Key Laboratory for Chemistry and Molecular Engineering of Medicinal Resources, School of Chemistry and Pharmaceutical Sciences of Guangxi Normal University, Guilin 541004, People's Republic of China*

Yan Cao − *State Key Laboratory for Chemistry and Molecular Engineering of Medicinal Resources, School of Chemistry and Pharmaceutical Sciences of Guangxi Normal University, Guilin 541004, People's Republic of China*

Tai-Xue Wu − *State Key Laboratory for Chemistry and Molecular Engineering of Medicinal Resources, School of Chemistry and Pharmaceutical Sciences of Guangxi Normal University, Guilin 541004, People's Republic of China*

https://doi.org/10.1021/acscatal.1c01996
ACS Catal. 2021, 11, 6944−6950

Ye Tao − *State Key Laboratory for Chemistry and Molecular Engineering of Medicinal Resources, School of Chemistry and Pharmaceutical Sciences of Guangxi Normal University, Guilin 541004, People's Republic of China*

Complete contact information is available at: https://pubs.acs.org/10.1021/acscatal.1c01996

Author Contributions

All author have given approval to the final version of the manuscript

Notes

The authors declare no competing financial interest.

■ ACKNOWLEDGMENTS

We thank the National Natural Science Foundation of China (21861006, 22061003, 22075056, 21861005), Guangxi Natural Science Foundation of China (2019GXNSFAA245027), Guangxi Key R&D Program (No. AB18221005), BAGUI Scholar Program of Guangxi Province of China (2016A13), Guangxi science and technology base and special talents (guike AD19110027), and State Key Laboratory for Chemistry and Molecular Engineering of Medicinal Resources (CMEMR2020-A13) for financial support. We also thank Prof. Chun-Zhi Ai of Guangxi Normal University for her help in DFT calculation.

■ REFERENCES

(1) (a) Hiyama, T.; Kusumoto, T. In *Comprehensive Organic Synthesis*; Trost, B. M., Fleming, I., Eds.; Pergamon Press: Oxford, 1991; Vol. *8*, pp 763−792. (b) Oshima, K. In *Science of Synthesis*; Fleming, I., Ed.; Thieme: Stuttgart, Germany, 2002; Vol. *4*, pp 713−756. (c) Marciniec, B. *Silicon Chem.* **2002**, *1*, 155−174. (d) Trost, B. M.; Ball, Z. T. *Synthesis* **2005**, *2005*, 853−887.

(2) (a) Rémond, E.; Martin, C.; Martinez, J.; Cavelier, F. Silicon-containing amino acids: synthetic aspects, conformational studies, and applications to bioactive peptides. *Chem. Rev.* **2016**, *116*, 11654−11684. (b) Bracegirdle, S.; Anderson, E. A. Recent advances in the use of temporary silicon tethers in metal-mediated reactions. *Chem. Soc. Rev.* **2010**, *39*, 4114−4129.

(3) (a) Ojima, I.; Li, Z.; Zhu, J. In *The Chemistry of Organosilicon Compounds*; Rappoport, S., Apeloig, Y., Eds.; Wiley: New York, 1998. (b) Langkopf, E.; Schinzer, D. *Chem. Rev.* **1995**, *95*, 1375−1408.

(4) (a) Fleming, I.; Barbero, A.; Walter, D. *Chem. Rev.* **1997**, *97*, 2063. (b) Denmark, S. E.; Sweis, R. F. *Metal-Catalyzed Cross-Coupling Reactions*, 2nd ed.; Wiley-VCH: Weinheim, 2008; p 163.

(5) (a) *Hydrosilylation: A Comprehensive Review on Recent Advances*; Marciniec, B., Ed.; Springer: Berlin, 2009. (b) Roy, A. K. A review of recent progress in catalyzed homogeneous hydrosilation (hydrosilylation). *Adv. Organomet. Chem.* **2007**, *55*, 1−59. (c) Brunner, H. A New Hydrosilylation Mechanism-New Preparative Opportunities. *Angew. Chem., Int. Ed.* **2004**, *43*, 2749−2750. (d) Lim, D. S.; Anderson, E. A. Synthesis of vinylsilanes. *Synthesis* **2012**, *44*, 983−1010. (e) Sun, J.; Deng, L. Cobalt complex-catalyzed hydrosilylation of alkenes and alkynes. *ACS Catal.* **2016**, *6*, 290−300.

(6) (a) Wu, C.; Teo, W. J.; Ge, S. Cobalt-catalyzed (*E*)-selective *anti*-Markovnikov hydrosilylation of terminal alkynes. *ACS Catal.* **2018**, *8*, 5896−5900. (b) Guo, J.; Wang, H.; Xing, S.; Hong, X.; Lu, Z. Cobalt-Catalyzed Asymmetric Synthesis of *gem*-Bis (silyl) alkanes by Double Hydrosilylation of Aliphatic Terminal Alkynes. *Chem.* **2019**, *5*, 881−895. (c) Guo, J.; Shen, X.; Lu, Z. Regio- and enantioselective cobalt-catalyzed sequential hydrosilylation/hydrogenation of terminal alkynes. *Angew. Chem., Int. Ed.* **2017**, *56*, 615−618. (d) Guo, J.; Lu, Z. Highly chemo-, regio-, and stereoselective cobalt-catalyzed markovnikov hydrosilylation of alkynes. *Angew. Chem., Int. Ed.* **2016**, *55*, 10835−10838. (e) Wang, Z.-L.; Zhang, F.-L.; Xu, J.-L.; Shan, C.-C.; Zhao, M.; Xu, Y.-H. Copper-Catalyzed Anti-Markovnikov Hydrosilylation of Terminal Alkynes. *Org. Lett.* **2020**, *22*, 7735−7742. (f) Li, R.-H.; An, X.-M.; Yang, Y.; Li, D.-C.; Hu, Z.-L.; Zhan, Z.-P. Highly Regio- and Stereoselective Heterogeneous Hydrosilylation of Terminal Alkynes over Cobalt-Metalated Porous Organic Polymer. *Org. Lett.* **2018**, *20*, 5023−5026. (g) Wang, H.; Huang, Y.; Wang, X.; Cui, X.; Shi, F. Supported Ni nanoparticles with a phosphine ligand as an efficient heterogeneous non-noble metal catalytic system for regioselective hydrosilylation of alkynes. *Org. Biomol. Chem.* **2020**, *18*, 7554−7558.

(7) (a) Zhao, X.; Yang, D.; Zhang, Y.; Wang, B.; Qu, J. Highly β (*Z*)-Selective Hydrosilylation of Terminal Alkynes Catalyzed by Thiolate-Bridged Dirhodium Complexes. *Org. Lett.* **2018**, *20*, 5357−5361. (b) Lim, D. S.; Anderson, E. A. Synthesis of vinylsilanes. *Synthesis* **2012**, *44*, 983−1010. (c) Kawanami, Y.; Sonoda, Y.; Mori, T.; Yamamoto, K. Ruthenium-catalyzed hydrosilylation of 1-alkynes with novel regioselectivity. *Org. Lett.* **2002**, *4*, 2825−2827. (d) Trost, B. M.; Ball, Z. T. Alkyne hydrosilylation catalyzed by a cationic ruthenium complex: efficient and general trans addition. *J. Am. Chem. Soc.* **2005**, *127*, 17644−17655.

(8) Docherty, J. H.; Peng, J.; Dominey, A. P.; Thomas, S. P. Activation and discovery of earth-abundant metal catalysts using sodium *tert*-butoxide. *Nat. Chem.* **2017**, *9*, 595.

(9) Zuo, Z.; Yang, J.; Huang, Z. Cobalt-catalyzed alkyne hydrosilylation and sequential vinylsilane hydroboration with Markovnikov selectivity. *Angew. Chem., Int. Ed.* **2016**, *55*, 10839−10843.

(10) Zhang, S.; Ibrahim, J. J.; Yang, Y. An NNN-Pincer-Cobalt Complex Catalyzed Highly Markovnikov-Selective Alkyne Hydrosilylation. *Org. Lett.* **2018**, *20*, 6265−6269.

(11) Zong, Z.; Yu, Q.; Sun, N.; Hu, B.; Shen, Z.; Hu, X.; Jin, L. Bidentate Geometry-Constrained Iminopyridyl Ligands in Cobalt Catalysis: Highly Markovnikov-Selective Hydrosilylation of Alkynes. *Org. Lett.* **2019**, *21*, 5767−5772.

(12) (a) Wu, G.; Chakraborty, U.; von Wangelin, A. J. Regiocontrol in the cobalt-catalyzed hydrosilylation of alkynes. *Chem. Commun.* **2018**, *54*, 12322−12325. (b) Kong, D.; Hu, B.; Chen, D. Highly Regio- and Stereoselective Hydrosilylation of Alkynes Catalyzed by Tridentate Cobalt Complexes. *Chem. - Asian J.* **2019**, *14*, 2694−2703.

(13) Cano, R.; Yus, M.; Ramón, D. J. Impregnated platinum on magnetite as an efficient, fast, and recyclable catalyst for the hydrosilylation of alkynes. *ACS Catal.* **2012**, *2*, 1070−1078.

(14) Zhou, Y.-B.; Liu, Z.-K.; Fan, X.-Y.; Li, R.-H.; Zhang, G.-L.; Chen, L.; Pan, Y.-M.; Tang, H.-T.; Zeng, J.-H.; Zhan, Z.-P. Porous Organic Polymer as a Heterogeneous Ligand for Highly Regio- and Stereoselective Nickel-Catalyzed Hydrosilylation of Alkyne. *Org. Lett.* **2018**, *20*, 7748−7752.

(15) (a) Zhang, Z.-M.; Yao, S.; Li, Y.-G.; Clérac, R.; Lu, Y.; Su, Z.-M.; Wang, E.-B. Protein-sized chiral Fe_{168} cages with NbO-type topology. *J. Am. Chem. Soc.* **2009**, *131*, 14600−14601. (b) Tasiopoulos, A. J.; Vinslava, A.; Wernsdorfer, W.; Abboud, K. A.; Christou, G. Giant single-molecule magnets: a $\{Mn_{84}\}$ torus and its supramolecular nanotubes. *Angew. Chem., Int. Ed.* **2004**, *43*, 2117−2121. (c) Alborés, P.; Rentschler, E. A Co_{36} Cluster Assembled from the Reaction of Cobalt Pivalate with 2,3-Dicarboxypyrazine. *Angew. Chem., Int. Ed.* **2009**, *48*, 9366−9370. (d) Ji, J.; Wang, G.; Wang, T.; You, X.; Xu, X. Thiolate-protected Ni_{39} and Ni_{41} nanoclusters: synthesis, self-assembly and magnetic properties. *Nanoscale* **2014**, *6*, 9185−9191. (e) Zhao, B.; Zhang, R.; Huang, Z.; Wang, B. Effect of the size of Cu clusters on selectivity and activity of acetylene selective hydrogenation. *Appl. Catal., A* **2017**, *546*, 111−121.

(16) (a) Craig, G. A.; Murrie, M. 3d single-ion magnets. *Chem. Soc. Rev.* **2015**, *44*, 2135−2147. (b) Nguyen, T. N.; Shiddiq, M.; Ghosh, T.; Abboud, K. A.; Hill, S.; Christou, G. Covalently linked dimer of Mn_3 single-molecule magnets and retention of its structure and quantum properties in solution. *J. Am. Chem. Soc.* **2015**, *137*, 7160−7168.

(17) (a) Jin, Y.; Li, S.; Han, Z.; Yan, B.-J.; Li, H.-Y.; Dong, X.-Y.; Zang, S.-Q. Cations Controlling the Chiral Assembly of Luminescent Atomically Precise Copper (I) Clusters. *Angew. Chem., Int. Ed.* **2019**, *58*, 12143−12148. (b) Kobayashi, F.; Ohtani, R.; Teraoka, S.;

Yoshida, M.; Kato, M.; Zhang, Y.; Lindoy, L. F.; Hayami, S.; Nakamura, M. Phosphorescence at Low Temperature by External Heavy-Atom Effect in Zinc (II) Clusters. *Chem. - Eur. J.* **2019**, *25*, 5875−5879. (c) Zeng, M.-H.; Yin, Z.; Liu, Z.-H.; Xu, H.-B.; Feng, Y.-C.; Hu, Y.-Q.; Chang, L.-X.; Zhang, Y.-X.; Huang, J.; Kurmoo, M. Assembly of a Highly Stable Luminescent Zn_5 Cluster and Application to Bio-Imaging. *Angew. Chem., Int. Ed.* **2016**, *55*, 11407−11411.

(18) (a) Maayan, G.; Gluz, N.; Christou, G. A bioinspired soluble manganese cluster as a water oxidation electrocatalyst with low overpotential. *Nat. Catal.* **2018**, *1*, 48. (b) Hadt, R. G.; Hayes, D.; Brodsky, C. N.; Ullman, A. M.; Casa, D. M.; Upton, M. H.; Nocera, D. G.; Chen, L. X. X-ray spectroscopic characterization of Co (IV) and metal-metal interactions in Co_4O_4: Electronic structure contributions to the formation of high-valent states relevant to the oxygen evolution reaction. *J. Am. Chem. Soc.* **2016**, *138*, 11017−11030. (c) Ghosh, T.; Maayan, G. Efficient Homogeneous Electrocatalytic Water Oxidation by a Manganese Cluster with an Overpotential of Only 74 mV. *Angew. Chem.* **2019**, *131*, 2811−2816. (d) Cai, D.; Han, A.; Yang, P. Y.; Wu, Y.-F.; Du, P.; Kurmoo, M.; Zeng, M.-H. Heptanuclear Co, Ni and mixed Co-Ni clusters as high-performance water oxidation electrocatalysts. *Electrochim. Acta* **2017**, *249*, 343−352.

(19) (a) Baslé, A.; Platsaki, S.; Dennison, C. Visualizing Biological Copper Storage: The Importance of Thiolate-Coordinated Tetranuclear Clusters. *Angew. Chem., Int. Ed.* **2017**, *56*, 8697−8700. (b) Ebrahimi, K. H.; Silveira, C.; Todorovic, S. Evidence for the synthesis of an unusual high spin (S = 7/2)[Cu-3Fe-4S] cluster in the radical-SAM enzyme RSAD2 (viperin). *Chem. Commun.* **2018**, *54*, 8614−8617. (c) Fujishiro, T.; Terahata, T.; Kunichika, K.; Yokoyama, N.; Maruyama, C.; Asai, K.; Takahashi, Y. Zinc-ligand swapping mediated complex formation and sulfur transfer between SufS and SufU for iron-sulfur cluster biogenesis in *Bacillus subtilis*. *J. Am. Chem. Soc.* **2017**, *139*, 18464−18467.

(20) (a) Vogiatzis, K. D.; Polynski, M. V.; Kirkland, J. K.; Townsend, J.; Hashemi, A.; Liu, C.; Pidko, E. A. Computational approach to molecular catalysis by 3d transition metals: challenges and opportunities. *Chem. Rev.* **2019**, *119*, 2453−2523. (b) Yano, J.; Yachandra, V. Mn_4Ca cluster in photosynthesis: where and how water is oxidized to dioxygen. *Chem. Rev.* **2014**, *114*, 4175−4205.

(21) (a) Brown, C. J.; Toste, F. D.; Bergman, R. G.; Raymond, K. N. Supramolecular catalysis in metal-ligand cluster hosts. *Chem. Rev.* **2015**, *115*, 3012−3035. (b) Chen, Y.-Z.; Zhang, R.; Jiao, L.; Jiang, H.-L. Metal-organic framework-derived porous materials for catalysis. *Coord. Chem. Rev.* **2018**, *362*, 1−23. (c) Jiao, L.; Seow, J. Y. R.; Skinner, W. S.; Wang, Z. U.; Jiang, H.-L. Metal-organic frameworks: Structures and functional applications. *Mater. Today* **2019**, *27*, 43−68.

(22) (a) Zhu, L.; Liu, X.-Q.; Jiang, H.-L.; Sun, L.-B. Metal-organic frameworks for heterogeneous basic catalysis. *Chem. Rev.* **2017**, *117*, 8129−8176. (b) O'Keeffe, M.; Yaghi, O. M. Deconstructing the crystal structures of metal-organic frameworks and related materials into their underlying nets. *Chem. Rev.* **2012**, *112*, 675−702. (c) Jiao, L.; Wang, Y.; Jiang, H.-L.; Xu, Q. Metal-organic frameworks as platforms for catalytic applications. *Adv. Mater.* **2018**, *30*, 1703663.

(23) (a) Yu, R. P.; Hesk, N.; Rivera, N.; Pelczer, I.; Chirik, P. J. Iron-catalysed tritiation of pharmaceuticals. *Nature* **2016**, *529*, 195. (b) Palmer, W. N.; Chirik, P. J. Cobalt-Catalyzed Stereoretentive Hydrogen Isotope Exchange of $C(sp^3)$-H Bonds. *ACS Catal.* **2017**, *7*, 5674−5678.

(24) (a) Mo, Z.; Xiao, J.; Gao, Y.; Deng, L. Regio- and Stereoselective Hydrosilylation of Alkynes Catalyzed by Three-Coordinate Cobalt(I) Alkyl and Silyl Complexes. *J. Am. Chem. Soc.* **2014**, *136*, 17414. (b) Atienza, C. C. H.; Diao, T.; Weller, K. J.; Nye, S. A.; Lewis, K. M.; Delis, J. G.; Boyer, J. L.; Roy, A. K.; Chirik, P. J. Bis (imino) pyridine cobalt-catalyzed dehydrogenative silylation of alkenes: scope, mechanism, and origins of selective allylsilane formation. *J. Am. Chem. Soc.* **2014**, *136*, 12108−12118. (c) Cheng, B.; Lu, P.; Zhang, H.; Cheng, X.; Lu, Z. Highly Enantioselective Cobalt-Catalyzed Hydrosilylation of Alkenes. *J. Am. Chem. Soc.* **2017**, *139*, 9439−9442. (d) Cheng, B.; Liu, W.; Lu, Z. Iron-Catalyzed Highly Enantioselective Hydrosilylation of Unactivated Terminal Alkenes. *J. Am. Chem. Soc.* **2018**, *140*, 5014−5017.

(25) (a) Jun, C.-H.; Crabtree, R. H. Dehydrogenative silation, isomerization and the control of *syn*- vs. *anti*-addition in the hydrosilation of alkynes. *J. Organomet. Chem.* **1993**, *447*, 177−187. (b) Ojima, I.; Clos, N.; Donovan, R. J.; Ingallina, P. Hydrosilylation of 1-hexyne catalyzed by rhodium and cobalt-rhodium mixed-metal complexes. Mechanism of apparent trans addition. *Organometallics* **1990**, *9*, 3127−3133.

https://doi.org/10.1021/acscatal.1c01996
ACS Catal. 2021, 11, 6944−6950